Linear and nonlinear optical susceptibilities of Maxwell Garnett composites: Dipolar spectral theory

Mark I. Stockman* and Konstantin B. Kurlayev
Department of Physics and Astronomy, Georgia State University, Atlanta, Georgia 30303

Thomas F. George
Office of the Chancellor and Departments of Chemistry and Physics & Astronomy, University of Wisconsin-Stevens Point, Stevens Point, Wisconsin 54481

(Received 18 March 1999; revised manuscript received 5 August 1999)

A theory of linear and nonlinear optical susceptibilites of disordered composites consisting of nanospheres in a dielectric host (Maxwell Garnett composites) is developed. The theory is based on a spectral representation in the dipole approximation. Numerical computations are performed in the framework of the dipolar spectral theory to obtain the linear dielectric function and third-order hypersusceptibility. For the fill factors f (from 0.001 to 0.12) considered, our spectral function agrees within the expected 10% error with the previously published function. We have introduced a material independent spectral representation for hypersusceptibilities. The third-order hypersusceptibility $\chi_c^{(3)}$ shows regions of strong enhancement (by up to four orders of magnitude for a silver composite). The mean-field theory provides a reasonable approximation only at very low fill factors ($f \lesssim 10^{-3}$). For $f \gtrsim 0.04$, the mean-field theory fails dramatically almost everywhere, except for distant wings of the spectral contour (very far from optical resonances). A physical effect responsible for the failure of the mean-field theories and contributing to the resonant enhancement of nonlinear susceptibilities is large fluctuations of local fields in the resonant region. [S0163-1829(99)01748-8]

I. INTRODUCTION

The problem of optical (dipolar) susceptibilities of composites is a long-standing one in physics going back to such names as Lorentz,[1] Maxwell Garnett,[2] Brugemann,[3] and Lorentz.[4] Generally, the problem is formulated in the following way. The composite's geometry is given, and the dielectric functions and nonlinear susceptibilities of all components of the composite are specified. In most cases, a characteristic size of the geometrical features of the composite is much smaller than optical wavelengths, so that the composite as a whole is viewed as an optically homogeneous medium. The problem is to find the dielectric function and nonlinear susceptibilities of that composite medium.

The Maxwell Garnett (MG) geometry is the one where small inclusion particles, usually nanospheres, are embedded in a homogeneous host medium with different dielectric properties. In this paper we consider this geometry and not that of Brugemann, where two components of the composites are treated equally (either of those can be considered as the host or inclusion component).

The effect of composite microgeometry (or, rather, nanogeometry) is often described as that of local fields, i.e., electric fields induced by an exciting radiation at each of the inclusions that are different from the macroscopic (average) field in the composite. We consider disordered composites whose geometry is random. For a MG composite, this means that the positions of the inclusions are random. For such a composite, the local fields at every inclusion are random as a consequence of the structural disorder. If a theory neglects such a randomness, i.e., treats all inclusions as being equivalent, we call it a mean-field theory. We emphasize that local fields in a mean-field theory are still functions of coordinates $\mathbf{r}$ in space around an inclusion.

Conventionally in mean-field theories, the effects of local fields are expressed in terms of the Lorentz field,[1,4] a uniform field that exists in the Lorentz cavity surrounding an inclusion. This field may exceed the macroscopic field, causing enhancement of optical responses. Recently, the validity of results obtained using the Lorentz field concept has been re-evaluated on the basis of a Green's-function approach by Lagendijk and co-workers.[5,6] This research showed that the Lorentz-Lorenz formula, or its equivalents such as the Lorentz relation and Maxwell Garnett formula, can be obtained consistently using the so-called *independent scattering approximation*. This approach carries out the summation of diagrams containing as many inclusions as required, but takes each inclusion into account only once. The theory of Refs. 5 and 6 does not invoke such approximations of uncontrollable accuracy as mean-field approaches or decoupling of higher-order correlation functions. Our results obtained in the present paper, however, show that for a disordered composite the Maxwell Garnett formula (or its equivalents) fails in a resonant region where optical absorption is present. A more realistic analytic theory by Barrera *et al.*[7] was developed based on a diagrammatic approach to an expansion of the inverse matrix (resolvent) of coupled-dipole equations. This theory extends beyond the mean-field approximation. It depends on several approximations, among which is factorization of averages of powers (equivalent to some decoupling of higher correlations) and a selection of diagrams in Dyson-type equations. With these approximations, the theory of Ref. 7 is in good agreement with earlier computer simulations.[8,9] We also note that Refs. 5–9 do not consider nonlinear optical responses.

A number of published studies devoted to calculations of linear responses of composites have been based on spectral expansion method by Bergman,[10,11] Bergman and Stroud,[12] Milton,[13] and Fuchs, Claro, Barrera, Rojas, and Castillo.[14–17] In this paper we will use our dipolar spectral approach,[18] which is a modification of the general spectral approach adapted for systems described by the dipole approximation (see below in Sec. II B). Solutions in the dipolar spectral expansion exactly obey general relations such as the optical theorem, dipole sum rule, etc. This automatic compliance with exact properties is due only to the form of the spectral expansion and orthonormality and completeness of the eigenvector set. This fact contributes to the numerical stability of our computations.

In any spectral approach, geometrical and material properties of the composite are completely separated. The linear responses of a composite are defined by spectral function $g(s)$ that depends only on geometry, but not on the composition of a composite. The composition determines only the value of the spectral parameter s in the integral expression for the susceptibility.[12] For the Maxwell Garnett type of composites, the spectral function has been calculated by Hinsen and Felderhof[19] using multipoles up to $l=4$ for the fill factor of the composite $f\leqslant 0.5$. We will compare these results to ours in this paper (in Sec. III B).

The dipolar spectral expansion also provides a powerful method of numerical solution of the problem that we use in the present paper. The advantage of such a method is its numerical stability. This is owed to a significant degree to the fact that the exact analytical properties of the solution are already taken into account by the mere structure of the spectral expansion, which is preserved irrespectively of the numerical precision achieved.

Nonlinear optical responses of a Maxwell Garnett composite for an arbitrary polarization of light have been calculated by Sipe and Boyd.[20] Their paper consistently described local (mesoscopic) fields inside a composite varying in space, but did not take into account variations of those fields from one inclusion to another. Hence, in our classification, Ref. 20 is a mean-field theory. In the present paper, we also calculate the same responses in a different formulation of the mean-field approximation. The linear optical response and nonlinear responses for the case of nonlinearity in inclusions are identical to those of Ref. 20. In the case of a nonlinear host, our results are close, though not completely identical, to those of Ref. 20.

We also note that experimental investigations of optically nonlinear composites have recently been done.[21,22] The results obtained in Refs. 21 and 22 are interpreted on the basis of the theory of Ref. 20. We show in this paper that for fill factors of composites studied in Refs. 21 and 22, the mean-field approach is indeed a very good one.

Nonlinear susceptibilities of composites have been the subject of a number of studies.[12,23–26] It has been shown[12,23,24] that to find the third-order susceptibility $\chi^{(3)}$ for a *linearly* polarized light of a composite from those of its components, one has to know only the local (mesoscopic) field in the first order in the intensity, i.e., to solve only an optically-linear problem. The unknown nonlinear (third-order) field is explicitly eliminated using boundary conditions. We use this approach in our numerical calculations in the present paper.

Earlier we used the dipolar spectral expansion to find an enhancement of third-order nonlinear photoprocesses in clusters.[26,27] We showed that fluctuations of local fields in space are very large (giant),[27] and are a determining factor of nonlinear responses. Composites, that are the subject of the present paper, differ from clusters in two respects. First, a composite has a host medium that can also be optically nonlinear. Second, a composite is infinite in all directions. These distinctions are addressed in this paper. We do not use decoupling of higher-order products of fields as in Ref. 25, because such a decoupling would not correctly reproduce spatial fluctuations of the local fields established earlier.[27]

In Sec. II A we introduce mesoscopic and macroscopic fields, and obtain general integral expressions for linear and nonlinear optical responses. In Sec. II B we start from fundamental equations to derive the dipolar spectral representation for the required susceptibilities. In Sec. II C we obtain expressions for a hypersusceptibility $\chi_c^{(3)}$ of a composite in a mean-field approximation. In Sec. II D, in a mean-field approximation, we find a general third-order hypersusceptibility for a composite characterized by two parameters A_c and B_c. We compare the results obtained with an earlier study.[20] In Sec. III we present results of a detailed numerical investigation.

II. MESOSCOPIC THEORY OF SUSCEPTIBILITIES OF COMPOSITES

A. Integral formulas for optical responses

In this section we very briefly summarize general relations that we need to find optical susceptibilites. We introduce the mesoscopic field $\boldsymbol{e}=\boldsymbol{e}(\mathbf{r})$ and induction $\boldsymbol{d}=\boldsymbol{d}(\mathbf{r})$ that are functions of a coordinate $\mathbf{r}$ inside a composite. The corresponding macroscopic (completely averaged) quantities are denoted as $\mathbf{E}$ and $\mathbf{D}$,

$$\mathbf{E}=\frac{1}{V}\int_V \boldsymbol{e}(\mathbf{r})d^3r, \quad \mathbf{D}=\frac{1}{V}\int_V \boldsymbol{d}(\mathbf{r})d^3r, \tag{1}$$

where V is the volume of the composite. We consider the third-order optical nonlinearity that for an isotropic medium is defined by the following material relation between the field and induction,

$$\boldsymbol{d}=\varepsilon(\mathbf{r})\boldsymbol{e}(\mathbf{r})+4\pi\left[A(\mathbf{r})|\boldsymbol{e}(\mathbf{r})|^2\boldsymbol{e}(\mathbf{r})+\frac{B(\mathbf{r})}{2}\boldsymbol{e}^2(\mathbf{r})\boldsymbol{e}^*(\mathbf{r})\right],$$

$$\mathbf{D}=\varepsilon_c\mathbf{E}+4\pi\left[A_c|\mathbf{E}|^2\mathbf{E}+\frac{B_c}{2}\mathbf{E}^2\mathbf{E}^*\right], \tag{2}$$

where ε, A, and B are functions of the coordinates that acquire the values ε_i, A_i, B_i and ε_h, A_h, B_h in the inclusion particles and host, correspondingly, and ε_c, A_c, and B_c are similar macroscopic quantities for the composite (coordinate independent). We also emphasize that we consider optical (oscillating in time) electric fields. The notations $\boldsymbol{e}$, $\boldsymbol{d}$, $\mathbf{E}$, $\mathbf{D}$, etc. are used for time-independent *amplitudes* of these fields.

We impose a boundary condition on the mesoscopic electrostatic potential $\varphi(\mathbf{r})$ at the surface S of the composite,

$$\varphi(\mathbf{r})=\phi(\mathbf{r})|_{\mathbf{r}\in S}, \tag{3}$$

where $\phi(\mathbf{r})$ is the macroscopic potential. Everywhere in this paper, except for Sec. II D, we consider a linearly polarized (say, along the z direction) macroscopic field $\mathbf{E}$, so $\phi(\mathbf{r})=-Ez$. This corresponds to the quasistatic approximation, where $\mathbf{E}$ is a constant in space (but, of course, oscillates with the optical frequency in time). This approximation is valid if the size of the composite under consideration is much smaller than the wavelength of light.

Following Refs. 12, 23, and 24, by transforming from a bulk to surface integral over the boundary and back, one can easily derive an exact expression

$$D=\frac{1}{VE}\int_V \boldsymbol{d}(\mathbf{r})\boldsymbol{e}(\mathbf{r})d^3r. \tag{4}$$

In what follows, we will find solutions for potentials and fields as expansions over the optical nonlinearity,

$$\varphi=\varphi^{(1)}+\varphi^{(3)}+\cdots, \quad \boldsymbol{e}=\boldsymbol{e}^{(1)}+\boldsymbol{e}^{(3)}+\cdots, \tag{5}$$

where the index shows the order in the electric field amplitude. Correspondingly, the boundary condition (3) yields

$$\varphi^{(1)}(\mathbf{r})=\phi(\mathbf{r})|_{\mathbf{r}\in S}, \quad \varphi^{(3)}(\mathbf{r})=0|_{\mathbf{r}\in S}. \tag{6}$$

From this relation, using a (generalized) Gauss theorem, we derive that there is no third-order correction to the macroscopic field $\mathbf{E}$,

$$\mathbf{E}^{(3)}\equiv\frac{1}{V}\int_V \boldsymbol{e}^{(3)}(\mathbf{r})d^3r=0, \tag{7}$$

and, correspondingly, $\mathbf{E}^{(1)}=\mathbf{E}$. Similarly, one can show that there are no corrections to $\mathbf{E}$ in any order, so that the ''external'' field $\mathbf{E}$ is actually the exact macroscopic field. This is consistent with the boundary condition of Eq. (3) that sets the potential ϕ as the exact macroscopic potential.

Substituting Eq. (5) into Eq. (4) and using Eq. (6), we obtain, in first order, an expression for the dielectric function ε_c of the composite,

$$\varepsilon_c=\frac{1}{VE^2}\int_V \varepsilon(\mathbf{r})[\boldsymbol{e}^{(1)}(\mathbf{r})]^2\,d^3r. \tag{8}$$

Alternatively, the dielectric function of the composite can be found directly from the macroscopic (averaged) first-order induction as

$$\varepsilon_c=\frac{1}{VE}\int_V \varepsilon(\mathbf{r})e_z^{(1)}(\mathbf{r})d^3r. \tag{9}$$

Equation (9) is actually very convenient to express ε_c in a form suitable for numerical computations. To do so, we introduce the dipole moment on an ath inclusion particle:

$$\mathbf{d}_a=-\frac{1}{4\pi}\int_{V_a}\frac{1}{s(\mathbf{r})}\boldsymbol{e}^{(1)}(\mathbf{r})d^3r, \quad s(\mathbf{r})\equiv\frac{\varepsilon_h}{\varepsilon_h-\varepsilon_i(\mathbf{r})}. \tag{10}$$

This dipole moment $\mathbf{d}_a$ is related to the polarizability tensor $\alpha^{(a)}$ of an ath inclusion in the composite[28]:

$$d_{a\beta}=\alpha^{(a)}_{\beta\gamma}E_\gamma. \tag{11}$$

Here and below, the Greek indices in subscripts denote Cartesian components, $\beta,\gamma,\cdots=x,y,z$. Substituting the definitions of Eqs. (10) and (11) into Eq. (9), we arrive at the required expression for the dielectric function of the composite,

$$\varepsilon_c=\varepsilon_h\left(1+4\pi\frac{N}{V}\alpha\right), \quad \alpha=\frac{1}{3N}\sum_{a=1}^{N}\alpha^{(a)}_{\beta\beta}, \tag{12}$$

where α is the average polarizability of the inclusions, V is the volume of the composite, and N is the number of inclusions in the composite. Isotropicity, or the random orientation of the inclusions, is assumed to average over Cartesian indices. Here and below, the summation over recurring vector indices is implied.

Similarly, substituting the expansion of Eq. (5) into Eq. (4), using the generalized Gauss theorem to transform to a surface integral and back to the volume integral, and using the boundary conditions [Eq. (6)], for the third-order nonlinear terms, one obtains the known expression[12,23,24] for the hypersusceptibility of the composite $\chi_c^{(3)}\equiv A_c+\frac{1}{2}B_c$,

$$\chi_c^{(3)}=\frac{1}{V|E|^2E^2}\int_V \chi^{(3)}(\mathbf{r})|\boldsymbol{e}^{(1)}(\mathbf{r})|^2[\boldsymbol{e}^{(1)}(\mathbf{r})]^2\,d^3r, \tag{13}$$

where $\chi^{(3)}(\mathbf{r})=A(\mathbf{r})+\frac{1}{2}B(\mathbf{r})$ is the coordinate-dependent third-order susceptibility of the composite matter. A principal advantage of this expression is that the unknown third-order field $\boldsymbol{e}^{(3)}$ vanishes from Eq. (13) as a result of application of the boundary conditions. Only the linear (first-order) field $\boldsymbol{e}^{(1)}$ needs to be known to find the nonlinear susceptibility of the composite $\chi_c^{(3)}$. Equation (13) is actually used in our numeric computations.

Using Eq. (7) we can find the coefficients A_c and B_c of the composite nonlinear susceptibility through the average of the mesoscopic nonlinear polarization:

$$\begin{aligned}\mathbf{D}^{(3)}&\equiv 4\pi\left[A_c|\mathbf{E}|^2\mathbf{E}+\frac{B_c}{2}\mathbf{E}^2\mathbf{E}^*\right]\\&=\frac{1}{V}\int_V d^3r\left\{\varepsilon(\mathbf{r})\boldsymbol{e}^{(3)}(\mathbf{r})+4\pi\left[A(\mathbf{r})|\boldsymbol{e}^{(1)}(\mathbf{r})|^2\boldsymbol{e}^{(1)}(\mathbf{r})\right.\right.\\&\quad\left.\left.+\frac{B(\mathbf{r})}{2}\boldsymbol{e}^{(1)2}(\mathbf{r})\boldsymbol{e}^{(1)*}(\mathbf{r})\right]\right\}.\end{aligned} \tag{14}$$

A drawback of this equation comparing to Eq. (13) is that the unknown third-order correction to the field $\boldsymbol{e}^{(3)}(\mathbf{r})$ must be found. Its advantage is that it allows one to find both the coefficients A_c and B_c for the composite, not only their combination $\chi_c^{(3)}\equiv A_c+\frac{1}{2}B_c$ as in Eq. (13). We will use Eq. (14) in Sec. II D to find A_c and B_c in a mean-field approximation.

B. Dipolar spectral theory and susceptibilities of composites

In this section we briefly derive and summarize formulas of the dipolar spectral theory that constitute a basis for the numerical computations. To insure that all definitions are consistent with the expressions used in the numerical computations, we start with the potential-theory equations in the

form of Ref. 12 and then derive needed formulas in the dipolar spectral representation.[18]

The integral equation for the electric potential in the form of Ref. 12 is

$$\varphi(\mathbf{r})=\phi(\mathbf{r})+\int_V \frac{1}{s(\mathbf{r}')}\,\eta(\mathbf{r}')\,\frac{\partial G(\mathbf{r},\mathbf{r}')}{\partial r'_\gamma}\,\frac{\partial \varphi(\mathbf{r}')}{\partial r'_\gamma}\,d^3r', \tag{15}$$

where $\eta(\mathbf{r})$ equals 1 when $\mathbf{r}$ is inside any inclusion, and is zero otherwise, and $G(\mathbf{r},\mathbf{r}')$ is the Green's function for the Laplace operator and the boundary problem (3) under consideration. In particular, $G(\mathbf{r},\mathbf{r}')|_{r\in S}=0$, that insures the compliance of Eq. (15) with boundary condition (3).

Equation (15) can be rewritten in terms of the electric fields and a sum over inclusion particles,

$$e_\beta(\mathbf{r})=E_\beta+\frac{1}{4\pi}\sum_b \int_{V_b}\frac{1}{s(\mathbf{r}')}W_{\beta\gamma}(\mathbf{r},\mathbf{r}')e_\gamma(\mathbf{r}')d^3r', \tag{16}$$

where we have introduced the dipole-interaction tensor W:

$$W_{\beta\gamma}(\mathbf{r},\mathbf{r}')=-4\pi\frac{\partial}{\partial r_\beta}\frac{\partial}{\partial r'_\gamma}G(\mathbf{r},\mathbf{r}'). \tag{17}$$

For a composite large enough (the size of the composite greatly exceeding the typical separation between the inclusions), we can replace the Green's function by its expression for an infinite medium and obtain

$$W_{\beta\gamma}(\mathbf{r},\mathbf{r}')=\begin{cases}\dfrac{(\mathbf{r}-\mathbf{r}')^2\delta_{\beta\gamma}-3(\mathbf{r}-\mathbf{r}')_\beta(\mathbf{r}-\mathbf{r}')_\gamma}{|\mathbf{r}-\mathbf{r}'|^5}, & \mathbf{r}\neq\mathbf{r}'\\ 0, & \mathbf{r}=\mathbf{r}'.\end{cases} \tag{18}$$

Let us set $\mathbf{r}\in V_a$ (where V_a is the volume of an ith inclusion) in Eq. (16). Assuming that the inclusions are far from each other relative to their sizes, on the right-hand side of Eq. (16) for $b\neq a$, we can replace $W_{\beta\gamma}(\mathbf{r},\mathbf{r}')$ by $W_{\beta\gamma}(\mathbf{r},\mathbf{r}_b)$, where $\mathbf{r}_b$ is the position of the center of the bth inclusion, and, taking into account a definition of Eq. (10), we obtain

$$e_\beta(\mathbf{r})-\frac{1}{4\pi}\int_{V_a}\frac{1}{s(\mathbf{r}')}W_{\beta\gamma}(\mathbf{r},\mathbf{r}')e_\gamma(\mathbf{r}')d^3r'$$

$$=E_\beta-\sum_{b\neq a}W_{\beta\gamma}(\mathbf{r},\mathbf{r}_b)d_{b\gamma}. \tag{19}$$

The right-hand side of Eq. (19) has the meaning of a local field acting on the ath inclusion, and its left-hand side can be expressed in terms of the polarizability α_0 of an *isolated* inclusion. For simplicity, we will assume that all inclusions are identical in shape (spheres) and composition. This will transform Eq. (19) into the familiar form of the dipole-dipole interaction equation,

$$Zd_{a\beta}=E_\beta-\sum_{b=1}^{N}W_{\beta\gamma}(\mathbf{r}_a,\mathbf{r}_b)d_{b\gamma}, \tag{20}$$

where $Z=\alpha_0^{-1}$, and N is the number of inclusions. We also introduce the spectral variable X and dissipation parameter δ as[18]

$$X=-\operatorname{Re}Z,\quad \delta=-\operatorname{Im}Z, \tag{21}$$

which will be used below to obtain a material-independent description. For a uniform dielectric sphere of radius R_0 as an inclusion, for instance, we have

$$\alpha_0=R_0^3(\varepsilon_i-\varepsilon_h)/(\varepsilon_i+2\varepsilon_h). \tag{22}$$

We will follow the dipolar spectral theory developed in Refs. 18 and 29. For this purpose, we introduce $3N$-dimensional vectors $|d),|E),\ldots,$ with the components $(a\beta|d)=d_{a\beta}$, $(a\beta|E)=E_\beta$ (and similarly for other vectors) and obtain a single equation in a $3N$-dimensional space,

$$(Z+W)|d)=|E), \tag{23}$$

where the dipole-interaction operator is defined by its matrix elements as $(i\beta|W|j\gamma)=W_{\beta\gamma}(\mathbf{r}_i,\mathbf{r}_j)$. The main advantage of the spectral theory is the separation of the geometrical and material properties of a system. The latter enter the theory only through the parameter Z, while geometry is taken into account by the eigenvectors of Eq. (23).

The solution of Eq. (20) is determined by the eigenvalues w_n and eigenvectors (eigenmodes) $|n)$ of the W operator,[18]

$$(W-w_n)|n)=0, \tag{24}$$

where $n=1,\ldots,3N$ is the eigenmode's number. These eigenmodes are the surface plasmons in the whole composite.[18]

The solution of Eq. (23) is given by Eq. (11), where the polarizability $\alpha^{(a)}$ of an ath inclusion in the composite in the form of the spectral expansion[18] is

$$\alpha^{(a)}_{\beta\gamma}=\sum_b\left(a\beta\left|\frac{1}{Z+W}\right|b\gamma\right)=\sum_{n,b}(a\beta|n)(b\gamma|n)(Z+w_n)^{-1}. \tag{25}$$

The dielectric function of the composite [Eq. (12)] can be written in the spectral representation in Bergman's form[12]

$$\varepsilon=\varepsilon_h\left(1-\int\frac{g(u)}{s-u}du\right), \tag{26}$$

where Bergman's spectral variable $s=\varepsilon_h/(\varepsilon_h-\varepsilon_c)$ can be related to our variable Z as

$$s=\frac{1}{3}(1-R_0^3Z). \tag{27}$$

We note that the spectral function satisfies exact sum rules,[12]

$$\int_0^1\bar{g}(s)ds=1,\quad \bar{s}\equiv\int_0^1\bar{g}(s)s\,ds=\frac{1}{3}(1-f), \tag{28}$$

where $\bar{g}(s)\equiv(1/f)g(s)$ is the normalized spectral function, f is the fill factor, i.e., the fraction of the composite's volume occupied by inclusions, and $\bar{s}$ is the centroid of the spectral function. In the dipolar spectral theory,[18]

$$\bar{g}(X)=\lim_{\delta\to 0}\frac{1}{3\pi}\mathrm{Im}\sum_a \alpha^{(a)}_{\beta\beta}(Z). \tag{29}$$

This dipolar spectral function satisfies the sum rules[18] that in terms of the variable s have the forms

$$\int_0^1 \bar{g}(s)ds=1, \quad \bar{s}\equiv\int_0^1 \bar{g}(s)sds=\frac{1}{3}. \tag{30}$$

Comparison of Eqs. (28) and (30) confirms that the dipolar theory is the first nonvanishing approximation in the parameter $f\ll 1$, as one would expect. Consequently, the redshift of the centroid $\bar{s}$ of the spectral function with an increase of f is absent in the dipolar theory. Because of these inherent limitations of the dipolar theory, we limit ourselves to considering only small values of the fill factor ($f\leqslant 0.12$). Our results will then contain a relative error on the order of 10%, which is acceptable for the objectives of this paper. We compare our results for the *linear* responses with multipolar calculations of Ref. 19 in Sec. III B. This comparison confirms that for $f\leqslant 0.1$ there is a reasonably good qualitative agreement, in particular, the spectral broadening of the spectral function $\bar{g}(s)$ present in the dipolar theory is much greater than the shift of its centroid. This allows us to proceed with the main goal of this paper: consideration of the *nonlinear* susceptibilities, with confidence.

Let us now find the nonlinear optical responses of the composite. In the general case, both the inclusions and host are optically nonlinear. In this case, as follows from Eq. (13), the hypersusceptibility of the composite is the sum of hypersusceptibilities for both inclusions and the host in the composite. Therefore, we can consider those contributions separately.

In the case of nonlinear inclusions and an optically linear host (''internal nonlinearity''), assuming that these inclusions are uniform spheres of radius R_0, we find the linear (first-order) internal field $\boldsymbol{e}^{(1)}_a$ in an ath inclusion as

$$e^{(1)}_{a\beta}=q\alpha^{(a)}_{\beta\gamma}E_\gamma, \quad q\equiv\frac{1}{R_0^3}\frac{3\varepsilon_h}{\varepsilon_i-\varepsilon_h}. \tag{31}$$

Substituting this into Eq. (13) and assuming a linear (say, z) polarization of the macroscopic field $\mathbf{E}$, we arrive at a closed expression for the enhancement coefficient $g_i^{(3)}$ for the composite in the case of nonlinear inclusions:

$$g_i^{(3)}\equiv\frac{\chi_c^{(3)}}{\chi_i^{(3)}}=f|q|^2q^2\langle|\alpha^{(a)}_{\beta z}|^2(\alpha^{(a)}_{\gamma z})^2\rangle. \tag{32}$$

Here the fill factor of the composite, $f=V_i/V=(V-V_h)/V$, where V_i is the combined volume of all inclusion particles, and V_h is the total volume of the host not occupied by the inclusions. Here and below the angular brackets denote statistical averaging over random positions of the inclusions in the composite, and also over any other random variables in the system. In accord with the notations throughout in this paper, a subscript c denotes macroscopic quantities for the composite.

Now we consider the case of a nonlinear host, while the inclusions are considered as optically linear (''external nonlinearity''). In this case one cannot arrive at a closed expression of the type of Eq. (32) for the hypersusceptibility $\chi_c^{(3)}$ of the composite. Instead, we will compute $\chi_c^{(3)}$ numerically. A quantity needed for this computation is the mesoscopic linear field $\boldsymbol{e}^{(1)}(\mathbf{r})$ in the host. From Eq. (19), this field can be written in the form

$$e^{(1)}_\beta(\mathbf{r})=E_\beta-\sum_{b=1}^{N} W_{\beta\gamma}(\mathbf{r},\mathbf{r}_b)d_{b\gamma}. \tag{33}$$

Finally, we will find the hypersusceptibility by numerical integration over a region V_h occupied by the host (outside of the inclusions), cf. Eq. (13),

$$g_h^{(3)}\equiv\frac{\chi_c^{(3)}}{\chi_h^{(3)}}=\frac{1-f}{V_h|E|^2E^2}\int_{V_h}|\boldsymbol{e}^{(1)}(\mathbf{r})|^2[\boldsymbol{e}^{(1)}(\mathbf{r})]^2\,d^3r, \tag{34}$$

C. Composite's dielectric function ε_c and hypersusceptibility $\chi_c^{(3)}$ in mean-field approximation

To introduce the mean-field approximation, we use a coated sphere model. Here a spherical inclusion of radius R_0 consisting of a material with dielectric function ε_i is surrounded by a spherical shell of the host with dielectric function ε_h. The external radius of this shell is set to be R, where R is the mean radius of a volume containing one inclusion. By this definition, the fill factor $f=(R_0/R)^3$. The rest of the system, i.e., the region at $r>R$, is set to be the average composite medium with the dielectric function ε_c of the composite. The electric field in this composite medium is equal to the mean (macroscopic) uniform field $\mathbf{E}$ that determines the boundary condition at the host-composite interface. The boundary conditions at the two interfaces of the model (at $r=R_0$ and $r=R$) are the known electrostatic conditions[30] of continuity of the potential $\varphi(\mathbf{r})$ and of the normal component of induction, $\mathbf{r}\boldsymbol{d}(\mathbf{r})$.

Solving the electrostatic equations[30] in the linear approximation with the corresponding boundary conditions, we easily obtain the field in the inclusion, $\boldsymbol{e}_i^{(1)}(\mathbf{r})$ for $r\leqslant R_0$, and in the host, $\mathbf{e}_h^{(1)}(\mathbf{r})$ for $R\geqslant r>R_0$:

$$\boldsymbol{e}_i^{(1)}=\frac{3\varepsilon_h}{\varepsilon_i+2\varepsilon_h}\mathbf{E}_l, \quad \mathbf{E}_l\equiv\frac{\varepsilon_c+2\varepsilon_h}{3\varepsilon_h}\mathbf{E},$$

$$\boldsymbol{e}_h^{(1)}(\mathbf{r})=\mathbf{E}_l+\alpha_0\frac{3(\mathbf{r}\mathbf{E}_l)\mathbf{r}-r^2\mathbf{E}_l}{r^5}. \tag{35}$$

Here we have introduced the effective local (Lorentz) field $\mathbf{E}_l$, and the polarizability α_0 of an inclusion is given by Eq. (22). A self-consistency condition of Eq. (9), or, alternatively, the boundary conditions at the two interfaces of the problem, along with the solution of Eq. (35), yield the known Maxwell Garnett formula for the dielectric function of the composite, which we write in explicit form as

$$\varepsilon_c=\frac{1+2f\beta}{1-f\beta}, \quad \beta\equiv\frac{\alpha_0}{R_0^3}=\frac{\varepsilon_i-\varepsilon_h}{\varepsilon_i+2\varepsilon_h}. \tag{36}$$

For the mean-field model under consideration, a general formula (13) for the case of nonlinearity in the inclusions reduces to

$$\chi_c^{(3)}=\frac{3\chi_I^{(3)}}{4\pi R^3}\int_0^{R_0}\left|\frac{\boldsymbol{e}^{(1)}(\mathbf{r})}{E}\right|^2\left(\frac{\boldsymbol{e}^{(1)}(\mathbf{r})}{E}\right)^2 d^3r. \tag{37}$$

Substitution of the first of Eqs. (35) into Eq. (37) yields a known expression[20] for the hypersusceptibility of a composite in the mean-field approximation for the case of nonlinearity in the inclusions:

$$g_i^{(3)}\equiv\frac{\chi_c^{(3)}}{\chi_i^{(3)}}=f\left|\frac{\varepsilon_c+2\varepsilon_h}{\varepsilon_i+2\varepsilon_h}\right|^2\left(\frac{\varepsilon_c+2\varepsilon_h}{\varepsilon_i+2\varepsilon_h}\right)^2. \tag{38}$$

For the case of nonlinearity in the host, from Eq. (13) we obtain, for our model,

$$\chi_c^{(3)}=\frac{3\chi_h^{(3)}}{4\pi R^3}\int_{R_0}^{R}\left|\frac{\boldsymbol{e}^{(1)}(\mathbf{r})}{E}\right|^2\left(\frac{\boldsymbol{e}^{(1)}(\mathbf{r})}{E}\right)^2 d^3r. \tag{39}$$

Substituting the second of Eqs. (35) and performing some elementary but tedious integrations, we obtain, for the mean-field hypersusceptibility of the composite for the case of the nonlinear host,

$$\begin{aligned}g_h^{(3)}\equiv\frac{\chi_c^{(3)}}{\chi_h^{(3)}}=&\frac{1}{5}p^2|p|^2(1-f)[8f(1+f+f^2)|\beta|^2\beta^2\\&+6f(1+f)|\beta|^2\beta+2f(1+f)\beta^3\\&+18f(|\beta|^2+\beta^2)+5],\end{aligned} \tag{40}$$

where

$$p=\frac{\varepsilon_c+2\varepsilon_h}{3\varepsilon_h}. \tag{41}$$

Our equation (40) is somewhat different from the corresponding result of Sipe and Boyd [see Eq. (6.23) in Ref. 20] that can be written in the form

$$\begin{aligned}g_h^{(3)}\equiv\frac{\chi_c^{(3)}}{\chi_h^{(3)}}=&\frac{1}{5}|p|^2p^2[8f|\beta|^2\beta^2+6f|\beta|^2\beta+2f\beta^3\\&+18f(|\beta|^2+\beta^2)+5(1-f)].\end{aligned} \tag{42}$$

As one can conclude from comparison of Eqs. (40) and (42), the latter takes into account only the lowest power of the fill factor f. As a result of this, in particular, the expression of Eq. (42) does not tend to zero when the host vanishes, i.e., for $f\to 1$, which should hold for the case of optical nonlinearity in the host. At the same time, our equation (40) does clearly possess this property. We note, however, that this difference is less significant than it might seem to be, because one does not actually expect that either of the formulas in the limit of $f\to 1$ may be applicable to real systems.

D. Composite's hypersusceptibility parameters A_c and B_c in mean field approximation

In this section, in the framework of the mean-field approximation, we will find the coefficients A_c and B_c that completely characterize the hypersusceptibility of an isotropic composite for the case of external nonlinearity (i.e., nonlinear host and linear inclusions). These coefficients should be found in terms of the known coefficients A_h and B_h for the host. Though we will not use the composite coefficients A_c and B_c in the present numerical computations to compare them with results of the spectral theory, these coefficients by themselves are of interest because they provide a complete description of the third-order susceptibility of an isotropic composite. We will compare our result to the previous theory of Ref. 20, and show that they differ in terms proportional to higher powers of the filling factor f. Note that our result for the case of nonlinearity in inclusions (internal nonlinearity) does not differ from that of Ref. 20.

An electrostatic equation for the third-order field is $\partial\boldsymbol{d}^{(3)}(\mathbf{r})/\partial\mathbf{r}=0$. From this, taking Eqs. (2) and (5) into account, we obtain equations for the inclusion region, $r\leqslant R_0$,

$$\Delta\varphi^{(3)}(\mathbf{r})=0, \tag{43}$$

and for the host region, $R\geqslant r\geqslant R_0$,

$$\begin{aligned}\Delta\varphi^{(3)}(\mathbf{r})=\frac{4\pi}{\varepsilon_h}\Bigg[&A_h\boldsymbol{e}^{(1)}(\mathbf{r})\frac{\partial}{\partial\mathbf{r}}|\boldsymbol{e}^{(1)}(\mathbf{r})|^2\\&+\frac{B_h}{2}\boldsymbol{e}^{(1)*}(\mathbf{r})\frac{\partial}{\partial\mathbf{r}}[\boldsymbol{e}^{(1)}(\mathbf{r})]^2\Bigg],\end{aligned} \tag{44}$$

where $\boldsymbol{e}^{(1)}(\mathbf{r})$ is given by Eq. (35).

To find both the unknown hypersusceptibility coefficients A_c and B_c, we need to include at least two components in the macroscopic field, i.e., set $\mathbf{E}=\mathbf{e}_xE_x+\mathbf{e}_zE_z$. We seek the solution of Eqs. (43) and (44) as a spherical harmonic expansion

$$\varphi^{(3)}(\mathbf{r})=\sum_{lm}\sqrt{\frac{4\pi}{2l+1}}R_{lm}(r)Y_{lm}\left(\frac{\mathbf{r}}{r}\right), \tag{45}$$

where the summation over l is extended over $l=1$ and 3.

Substituting fields (35) into Eq. (44) and expanding over spherical harmonics, we obtain an equation for R_{10}, the only of the radial functions R_{lm} that we need to know,

$$\frac{1}{r}\frac{d^2[rR_{10}(r)]}{dr^2}-\frac{2R_{10}(r)}{r^2}=-18Q\left[\frac{g_1\beta|\beta|^2R_0^9}{r^{10}}+\frac{g_2R_0^6}{5r^7}\right], \tag{46}$$

where the notations are

$$Q=\frac{4\pi}{\varepsilon_h}p|p|^2,$$

$$\begin{aligned}g_1=&E_z(|E_x|^2+|E_z|^2)\left(\frac{3}{2}A_h+\frac{1}{2}B_h\right)\\&+E_z^*(E_x^2+E_z^2)\left(\frac{1}{2}A_h+\frac{1}{2}B_h\right),\end{aligned} \tag{47}$$

$$g_2 = E_z(|E_x|^2+|E_z|^2)\left[A_h\left(4|\beta|^2+\frac{1}{2}\beta^2\right)+\frac{1}{2}B_h(\beta^2+6|\beta|^2)\right]+E_z^*(E_x^2+E_z^2)\left[A_h\left(2|\beta|^2+\frac{3}{2}\beta^2\right)-\frac{1}{2}B_h(2|\beta|^2-3\beta^2)\right].$$

The solution of Eq. (46) has the form

$$R_{10}(r) = -\frac{1}{3}g_1 Q\beta|\beta|^2 R_0^9\frac{1}{r^8}-\frac{1}{5}g_2 Q R_0^6\frac{1}{r^5}+ar+b\frac{1}{r^2}, \tag{48}$$

where a and b are two coefficients of the general solution of the homogeneous equation that should be found from the boundary conditions.

Application of those conditions at $r=R$ results in the expressions

$$a = -\frac{2}{3}g_1 Q f^3\beta|\beta|^2-\frac{1}{5}g_2 Q f^2+\frac{1}{3}h,$$
$$b = R^3\left(g_1 Q f^3\beta|\beta|^2+\frac{2}{5}g_2 Q f^2-\frac{1}{3}h\right), \tag{49}$$

where the constant h is defined as

$$h = -\frac{4\pi}{\varepsilon_h}\left\{\left[A_c-A_h(1+S)\left(1+\frac{2}{5}(2\,\mathrm{Re}\,S+|S|^2)\right)-\frac{1}{5}B_h(1+S^*)(2S+S^2)\right]E_z(|E_x|^2+|E_z|^2)+\left[\frac{1}{2}B_c-\frac{1}{5}A_h(1+S)(2\,\mathrm{Re}\,S+|S|^2)-\frac{1}{2}B_h(1+S^*)\left(1+\frac{1}{5}(2S+S^2)\right)\right]E_z^*(E_x^2+E_z^2)\right\}, \tag{50}$$

and $S\equiv(\varepsilon_c-\varepsilon_h)/\varepsilon_h$.

The solution inside the inclusion (i.e., for $r\leqslant R_0$) obviously has the form

$$\varphi^{(3)}(\mathbf{r}) = \sum_{lm}\sqrt{\frac{4\pi}{2l+1}}R_{lm}(R_0)\left(\frac{r}{R_0}\right)^l Y_{lm}\left(\frac{\mathbf{r}}{r}\right). \tag{51}$$

To obtain this equation, we have used the boundary condition of potential continuity.

Applying the continuity condition for the normal component of induction $\boldsymbol{d}^{(3)}(\mathbf{r})$ for an interface at $r=R_0$ to Eqs. (45) and (51), we finally obtain the required expressions for A_c and B_c in terms of A_h and B_h:

$$A_c = p^2|p|^2(1-f)\left\{A_h\left[1+\frac{7}{5}f(1+f+f^2)\beta^2|\beta|^2+\frac{1}{10}f(1+f)\beta^3+\frac{3}{10}f(1+f)\beta|\beta|^2+\frac{12}{5}f(\beta^2+|\beta|^2)\right]+\frac{1}{2}B_h\left[\frac{2}{5}f(1+f+f^2)\beta^2|\beta|^2+\frac{3}{5}f(1+f)\beta^3+\frac{9}{5}f(1+f)\beta|\beta|^2+\frac{12}{5}f(\beta^2+|\beta|^2)\right]\right\}, \tag{52}$$

$$B_c = p^2|p|^2(1-f)\left\{B_h\left[1+\frac{6}{5}f(1+f+f^2)\beta^2|\beta|^2-\frac{1}{5}f(1+f)\beta^3-\frac{3}{5}f(1+f)\beta|\beta|^2+\frac{6}{5}f(\beta^2+|\beta|^2)\right]+A_h\left[\frac{2}{5}f(1+f+f^2)\beta^2|\beta|^2+\frac{3}{5}f(1+f)\beta^3+\frac{9}{5}f(1+f)\beta|\beta|^2+\frac{12}{5}f(\beta^2+|\beta|^2)\right]\right\}. \tag{53}$$

One can easily verify that the sum $A_c+B_c/2$ as given by Eqs. (52) and (53) does indeed reproduce the result of Eq. (40) obtained by an independent approach. Similar to Eq. (40), these values of A_c and B_c are not in a complete agreement with the corresponding result of Ref. 20: only terms containing the lowest powers of f agree [see Eq. (6.23) in Ref. 20]. Finally, we note that exactly the same result as in Eqs. (52) and (53) can be obtained by using the integral relation (14) instead of the boundary condition for $\boldsymbol{d}$.

III. NUMERICAL RESULTS

A. Numerical procedures

We have performed numerical computations of linear and nonlinear susceptibilities of Maxwell Garnett composites. The computations are based on the spectral theory as given by Eqs. (12), (25), (32), and (34). A considerable advantage of the spectral theory[18] is that the geometry of the composite and dielectric properties of its constituents are separated. In particular, the eigenvalue problem of Eqs. (18) and (24) depends only on *geometry* of the composite, while the spectral expansions for fields and polarizabilities depend on *dielectric properties* of the inclusions and host. This is a common advantage of spectral theories that is inherent in the general spectral theory.[12]

We have solved the eigenproblem (24) by known Lanczos algorithms[31] for large-scale diagonalization, and stored the eigenvectors and eigenvalues obtained. Once stored, these data have been used to compute spectral contours of composite's dielectric function and hypersusceptibility.

We have generated a composite by randomly placing spheres at sites of a cubic lattice. The radius R_0 of a sphere is arbitrarily set to equal 1. A specific value of R_0 only determines a reference scale for the spectral parameter X and the dissipation parameter δ of the theory [see Eqs. (21) and (22)]. We place from $N=75$ to 1500 spheres into the unit cell to achieve a fill factor from $f=0.001$ to 0.12. To de-

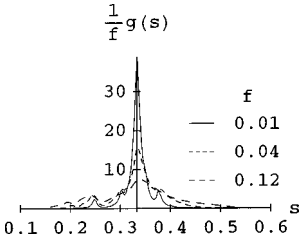

FIG. 1. Normalized spectral function $(1/f)g(s)$ for the values of the fill factor shown in the figure. The calculations are done for $N=500$ inclusion spheres per unit cell.

scribe an infinite composite, we impose periodic conditions at the boundary of the unit cell. This is equivalent to replacing the dipole tensor $W_{\beta\gamma}(\mathbf{r}_1,\mathbf{r}_2)$ in the formulas of Sec. II B by a periodic tensor $V_{\beta\gamma}(\mathbf{r}_1,\mathbf{r}_2)$ defined as

$$V_{\beta\gamma}(\mathbf{r}_1,\mathbf{r}_2)=\sum_{\mathbf{L}} W_{\beta\gamma}(\mathbf{r}_1,\mathbf{r}_2-\mathbf{L}), \tag{54}$$

where the sum is extended over all lattice vectors $\mathbf{L}$. The above-mentioned formulas (12), (25), (32), and (34) are still applicable if one understands that the summation over inclusions, $\Sigma_b \ldots$, is performed within the unit cell, N is the number of inclusions in that cell, V is its volume, and V_h is the volume occupied by the host in the unit cell.

Obviously, one cannot numerically compute the infinite sum in Eq. (54). In reality, this sum can be computed by either the known Ewald method (see, e.g., Ref. 32), or by simply truncating it at a large but finite number of repeated cells. We have employed the last approach. The unit cell is chosen as a cube, the lattice is cubic, and the truncated composite is a large cube. This procedure preserves the symmetry of the unit cell. The number of terms in the sum in Eq. (54) taken into account is from 13^3 to 25^3. We have carefully checked that this number of repeated cells is sufficient to achieve a targeted numerical precision (see Fig. 9 and the corresponding discussion in Sec. III D). From 150 to 1000 realizations of a random-composite unit cell have been generated by the Monte Carlo method, depending on the number of inclusions N used to achieve required statistical accuracy.

Numerical results to be discussed below are calculated in both the spectral form that is invariant with respect to the material composition of a composite and for a specific composition. That is, the specific computations are made for silver nanospheres in a hypothetical host whose dielectric constant is realistically chosen as $\varepsilon_h=2.0$. The optical constants of silver are taken from Ref. 33.

B. Dielectric function

The maximum information about linear susceptibility is contained in the spectral function $g(s)$; see Eq. (26). We show results of our computations of the normalized spectral function $\overline{g}(s)\equiv(1/f)g(s)$ in Fig. 1. As we see, the spectral function at small values of f is a narrow peak that broadens as f increases. The centroid of the peak stays at its position of $\overline{s}=\frac{1}{3}$ in accord with Eq. (30). In the corresponding results of Hinsen and Felderhof (see Fig. 4 in Ref. 19), the behavior is qualitatively similar except for a small shift of the centroid $\overline{s}$. Quantitatively, let us compare our results at the highest fill factor $f=0.12$ that we use (as the most difficult case for us). The height (maximum value) of our spectral function (Fig. 1) for $f=0.12$ is ≈ 8, while that of Ref. 19 is ≈ 9 for $f=0.1$. The red-wing edge of our spectral function is at $s=0.15$, and the same value one finds in Fig. 4 of Ref. 19 for $f=0.1$. The shift of the peak of $g(s)$ in Ref. 19 for $f=0.1$ is ≈ 0.015, an order of magnitude smaller than its half-width, as expected. This explains a reasonably good agreement (within ~ 10 percent) of the dipolar results of the present paper with multipolar results of Ref. 19 for the range of values $0.01\leqslant f\leqslant 0.12$ considered by us.

A quantitative distinction of $g(s)$ of Ref. 19 from Fig. 1 is somewhat larger amplitude of the oscillations seen in the spectral wings of both the results. These oscillations originate from interaction of the nearest neighbors and, therefore, should be different in the two theories because of the different small-scale order. In fact, our model is the lattice gas (randomly occupied sites on a regular lattice), while that of Ref. 19 is a hard-sphere gas with randomly positioned nonoverlapping spheres. We point out that the exact shape of the spectral function (amplitude of the oscillations, in particular) is not very important, because the actual susceptibility is obtained [cf. Eq. (26)] by the integration along a line shifted from the real axis due to dissipation ($\mathrm{Im}\, s$), which brings about smoothing of the spectral contour. Note that our choice of the random lattice-gas model is dictated by our intent to exclude closely packed neighbors, where the dipolar approximation might have failed.

Though the spectral function shown in Fig. 1 is sufficient to calculate the linear susceptibility of a composite with the given geometry and an arbitrary material composition, it is also useful to discuss trends susceptibilities and their relation to a mean-field theory as function of the fill factor f for a specific composite. As such, we chose a composite of silver spheres in a purely refracting (no dissipation) host of $\varepsilon_h=2.0$. We have chosen silver impurities because of the very low dissipation in silver in the red part of the visible spectrum. This leads to a number of resonant enhancement phenomena including giant enhancement of Raman scattering (see, e.g., the theory and comparison with experiment in Ref. 34).

In Fig. 2 we show the real and imaginary parts of the relative dielectric function of a composite $\epsilon\equiv\varepsilon_c/\varepsilon_h$ for the fill factor in the range $0.001\leqslant f\leqslant 0.12$ as functions of the light frequency ω (indicated as photon energy). Both the results of the present theory [see Eqs. (12) and (25)] and a mean field theory [Maxwell Garnett formula; see Eq. (36)] are plotted. As one can see, for small fill factors ($0.001\leqslant f\leqslant 0.01$), there is a good overall agreement between the present computations and Maxwell Garnett (mean-field) theory. With an increase of f to 0.04, this agreement deteriorates, especially for $\mathrm{Im}\,\epsilon$. While our computations, in agreement with Ref. 19, show a pronounced widening of the spectral profile, the Maxwell Garnett formula predicts a narrow peak moving very slightly toward the red wing. [We note that the Maxwell Garnett formula satisfies the exact sum rule (28) and, consequently, possesses the peak of absorption at the correct central frequency.] The same trend is even more pronounced for the highest fill factor of our computations, $f=0.12$.

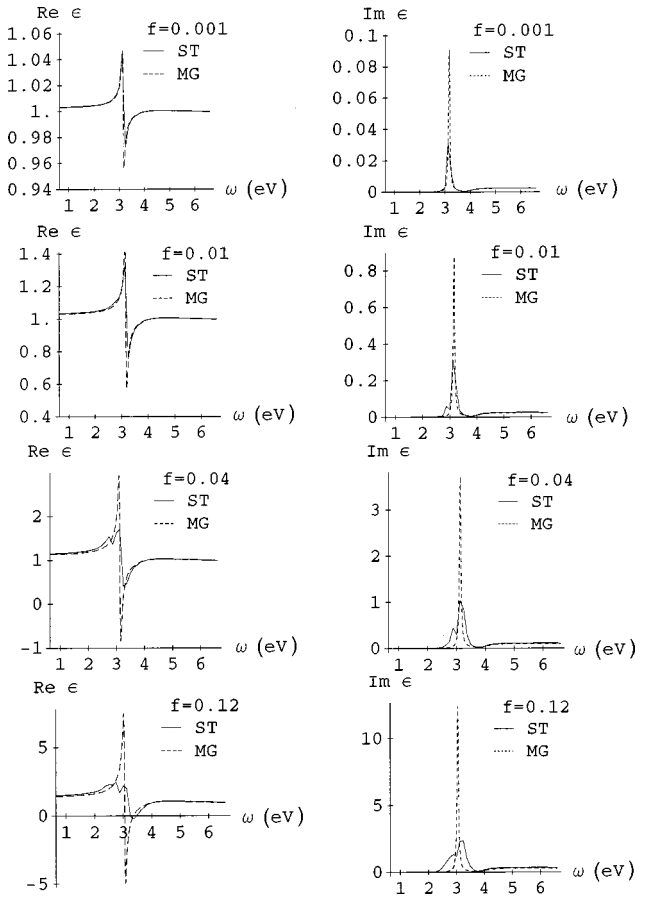

FIG. 2. Real (left column) and imaginary (right column) parts of the relative dielectric function of the composite, $\epsilon=\varepsilon_c/\varepsilon_h$, for the fill factors f shown in the graphs. The computations are done for $N=500$ inclusion spheres of silver in the unit cell. The solid lines denote the result of the present theory as given by Eqs. (12) and (25). The dashed line is a plot of the Maxwell Garnett formula for a composite with the same f and dielectric properties. The plots are given as functions of the photon energy (eV) for solid silver nanospheres as inclusions in a uniform host with $\varepsilon_h=2.0$.

Interestingly enough, for the real part of the susceptibility, the overall agreement with Maxwell Garnett formula is not bad even for $f=0.12$, except for the very central region of the absorption band. In that region, the Maxwell Garnett formula possesses a pole singularity. In contrast, in the present theory, there are multiple poles [every eigenvalue generates a weak pole; see Eq. (25)]. In the thermodynamic limit (the size of the system tends to infinity at a given fill factor), these poles overlap. This, most likely, leads to a weaker singularity, such as a branch cut. For this reason, the present theory does not predict ε_c to be as large in the resonant region as for the mean-field theory.

A singularity in the dielectric function (polarizability per inclusion in the composite) is of principal interest because its high values may lead to a dielectric instability. A similar effect is the formation of a gap in the density of states in doped semiconductors.[35] In our case, the condition of dielectric stability is that the maximum eigenvalue $|w_n|$ does not exceed the maximum possible (at any frequency) magnitude of the spectral variable $|X|$, or

$$\max|w_n| \leq \max \frac{1}{R_0^3}\left|\mathrm{Re}\,\frac{\varepsilon_i+2\varepsilon_h}{\varepsilon_i-\varepsilon_h}\right|. \tag{55}$$

Note that the spectrum w_n depends only on the geometry of the composite, and does not depend on R_0, ε_i, or ε_h. Obviously, the stability condition (55) can always be satisfied if the inclusions are small enough $(R_0 \to 0)$.

Any mean-field theory, the Maxwell Garnett theory in particular, requires that the mean field is much greater than the difference of the local fields at different inclusions. In other words, all inclusion should be equivalent, and *spatial* fluctuations of the local field measured at a given distance from any of the inclusions should be small compared to the fields themselves. Previously, we have shown that for *fractal* clusters the situation is completely opposite: the long-range nature of the dipole-dipole interaction causes giant spatial fluctuations of the local fields.[27] Undoubtedly, a similar situation should take place for fractal composites (i.e., composites with a fractal cluster in a host medium as the unit cell). A question is whether there are significant spatial fluctuations of local fields for a nonfractal Maxwell Garnett composite. The above-discussed results for the dielectric function suggest that those fluctuations should be large in the resonant (absorption) region.

To answer this question directly, we show in Fig. 3 the relative intensity of the local fields at different inclusions (more specifically, square of the local polarizability is the quantity plotted). One can see that indeed in the resonant region there are very strong (by orders of magnitude) changes of the local fields from one inclusion to another,

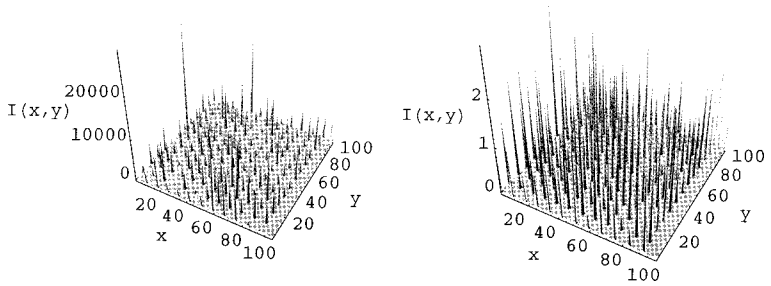

FIG. 3. Spatial distribution of the intensity of induced dipoles at different inclusions. This distribution is plotted in the following way: A composite is generated and local dipole polarizabilities $\alpha^{(a)}_{\beta\gamma}$ are found for each inclusion from Eq. (25). Then inclusions are projected onto the xy plane. If there are several inclusions projected onto the same site, one of them is randomly left. The square of the local polarizability $\frac{1}{3}|\alpha^{(a)}_{\beta z}|^2$ for each of the inclusions left is plotted as the vertical coordinate. The left panel shows the distribution for the resonant region (in terms of the spectral parameter $R_0^3X=-0.01$), while the right one is for the off-resonant region (spectral wing $R_0^3X=-1.0$).

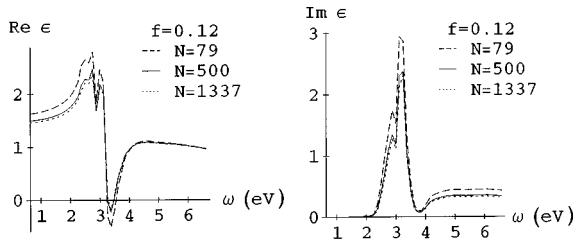

FIG. 4. Real (left panel) and imaginary (right panel) parts of the dielectric function ε_c of the composite for the fill factor $f=0.12$ and the indicated number N of inclusion spheres in the unit cell. The curves are shown as functions of the photon energy.

which we refer to as spatial fluctuations. In contrast, for an off-resonant region (see the right panel in Fig. 3), such fluctuations are much less pronounced. This explains why the Maxwell Garnett theory works in the spectral wings but fails in the central (resonant) region. One may expect that the effect of the spatial fluctuations on *nonlinear* susceptibilities will be much more significant. We show below that it indeed is the case.

Previously we have predicted giant fluctuations of local fields in fractal clusters and composites.[27] However, there is a major distinction between fractal and nonfractal composites: as we have shown above, the spatial fluctuations for a nonfractal Maxwell Garnett composite are strongest in the resonant region ($|X|\ll 1$), while for fractal composites they are most pronounced in a far-wing, off-resonant region ($|X|\gtrsim 1$). This difference notwithstanding, the fluctuating singular spatial distributions in Fig. 3 are similar to spatial distributions obtained earlier for inhomogeneously localized excitations in fractal clusters.[36–38]

In numerical computations with periodic boundary conditions there is always a question whether the size of the unit cell is sufficient. To answer this question, in Fig. 4 we present a plot of the dielectric function for a composite with the fill factor $f=0.12$ computed with different numbers of inclusions in the unit cell. As we see, the dependence on N levels off between $N=500$ and 1500, the two values used in the present calculations. The conclusion is that the size of the unit cell used is sufficient.

C. Hypersusceptibilities for composite with nonlinearity in inclusions

Now we consider the nonlinear (hyper)susceptibility $\chi^{(3)}$ in the case of a composite consisting of nonlinear inclusions embedded in an optically linear host. We performed computations for such composites with $N=500$ inclusions in the unit cell. Figure 5 presents the absolute values of the enhancement factor $g^{(3)}\equiv\chi^{(3)}/\chi_i^{(3)}$ calculated from the spectral theory [Eq. (32)] and from the mean-field theory [Eq. (38)] for fill factors in the range $0.001\leqslant f\leqslant 0.12$. For the very diluted composites ($f=0.001,0.01$), the spectral profile of $|g^{(3)}|$ consists of two peaks. The one at the absorption frequency (the right one of the two) is in reasonable agreement with the mean-field formula. However, there is also another considerable peak, redshifted from the absorption frequency. This peak has no counterpart in the mean-field curve. This shifted peak is due to the interaction between inclusions,

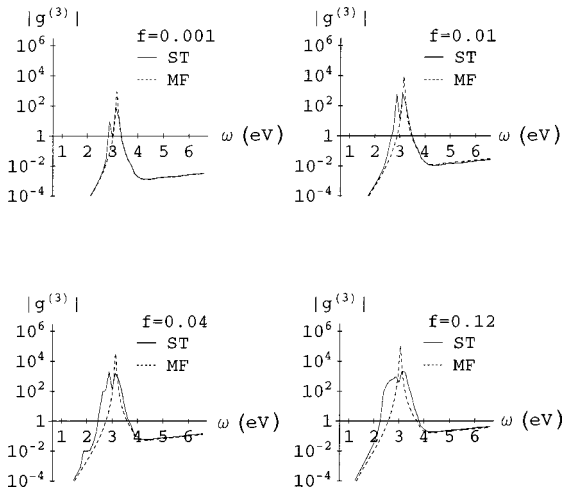

FIG. 5. Magnitude of the enhancement coefficient $|g^{(3)}|=|\chi_c^{(3)}/\chi_i^{(3)}|$ for nonlinear inclusions of silver in a linear host as a function of the photon energy for the fill factors shown in the figures. The solid curve is for the present spectral theory [Eq. (32)], and the dashed curve is for the mean-field theory [Eq. (38)]. The curves are plotted on a logarithmic scale.

which causes spatial fluctuations of the local fields and renders the mean-field approximation inapplicable. With an increase of f to the values of 0.04 and 0.12, the mean-field approximation fails completely, even on the order of magnitude, except for the very far wings of the spectral contour. The mean-field theory greatly overestimates $g^{(3)}$ in the region of the surface-plasmon resonance (at ≈ 3 eV) and underestimates $g^{(3)}$ farther away from this resonance. The present theory predicts a significant enhancement of the hypersusceptibility $\chi^{(3)}$, though this enhancement is much less than predicted[26,39] and observed[40] for fractal clusters (composites).

As we emphasized above in Secs. II B and III B, the spectral representation of the linear susceptibility has a great advantage of being material independent. In contrast to the linear case, the nonlinear susceptibilities directly depend on the dissipation in the medium. Therefore, one cannot directly generalize the spectral theory to the nonlinear case. Nevertheless, we will show below that the dependence on the dissipation can be parametrized in such a way that it acquires a universal scaling form in the most interesting part of the spectral region, where the enhancement of the nonlinear polarizability due to the composite structure is large.

The above-mentioned generalization can be implemented by expressing the enhancement factor $g^{(3)}$ as a function of the spectral variables X and δ. A plot of $|g^{(3)}(X)|$ for different values of δ is presented in Fig. 6 (note that the range of $\delta=0.001-0.1$ is realistic). As we see, for small $|X|$ the enhancement factor dependence levels off, reaching a maximum. As the plot in the right panel shows, the dependence on δ in the region $|X|\lesssim 1$ is scaling with a trivial index of -2, $|g^{(3)}|=C\delta^{-2}$, where C does not depend on δ. This result is the required spectral representation for the nonlinear susceptibility, which depends only on geometry but not on the material composition of a composite. At the same time, the universal (for a given geometry) dependence on the spectral parameters X and δ can be easily translated for any specific material into the dependence on light frequency using

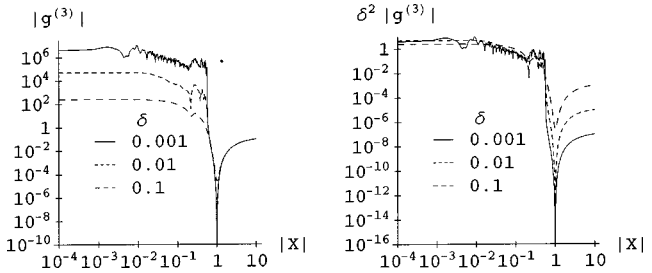

FIG. 6. Spectral representation of the nonlinear enhancement: Magnitude of the enhancement coefficient $|g^{(3)}|$ for the fill factor $f=0.12$ (500 inclusions of silver in the unit cell) for a linear host and nonlinear inclusions as functions of the spectral variable $|X|$ (the actual region plotted is for $X<0$, corresponding to visible light) for different values of the dissipation parameter δ (left panel). The right panel shows similar plots where $|g^{(3)}|$ is normalized by multiplication by δ^2. Note the double logarithmic scale.

the definition of Eq. (21). For instance, for silver the spectral parameters depend on the frequency as shown in Fig. 7.

It is interesting to note that for *fractal* clusters or composites, scaling in δ takes place in the opposite limiting case, for $|X|\gtrsim 1$, with an index of -3. We attribute this distinction to a different spectral distribution of the density of eigenmodes. In a Maxwell Garnett composite, a nonfractal system, eigenmodes are more abundant near the surface-plasmon resonance ($|X|\lesssim 1$), while in fractal systems a strong pair correlations brings about a shift of the eigenmode density toward larger $|X|$. This also leads to another principal distinction of a Maxwell Garnett composite from fractal systems. That is, the third-order enhancement in fractals actually *increases*, not decreases, with $|X|$, approximately, in a scaling manner,[39]

$$g^{(3)} \simeq \frac{|X|^3}{\delta^3}|X \operatorname{Im}\alpha| \simeq \frac{|X|^{3+d_0}}{\delta^3}, \tag{56}$$

where $1 \geqslant d_0 > 0$ is a nontrivial index, optical spectral dimension.

D. Hypersusceptibilities for composite with nonlinearity in host

Here we consider a case where the inclusions are optically linear, and all nonlinearity is in the host. One can expect that in this case a higher enhancement and lower dielectric losses can be achieved, because the outer electric field around a resonant dielectric sphere is higher than the internal field. The long range of the dipolar fields brings about strong mesoscopic fields in a large volume of the host around each of the inclusions. At the same time, optical absorption (dielectric losses) are concentrated in a relatively small volume of the inclusions. Below we test numerically these qualitative arguments.

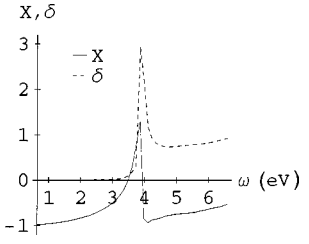

FIG. 7. Dependence of the spectral parameter X (solid line) and dissipation parameter δ (dashed line) on light frequency for a silver nanosphere.

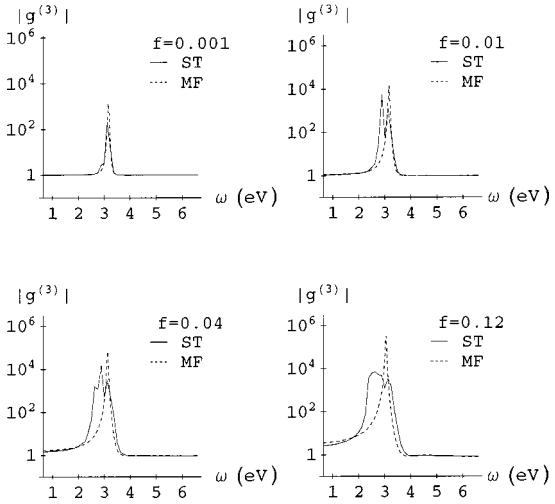

FIG. 8. Magnitude of the enhancement coefficient $|g^{(3)}| = |\chi_c^{(3)}/\chi_i^{(3)}|$ for optically linear inclusions of silver in the nonlinear host as functions of the photon energy for the fill factors shown in the figures. The solid curve is for the present theory [Eq. (32)], and the dashed curve is for the mean field theory [Eq. (40)]. The curves are plotted on a logarithmic scale.

The enhancement coefficient for the case under consideration $g^{(3)} \equiv \chi_c^{(3)}/\chi_h^{(3)}$ in the present theory has been calculated in accord with Eq. (34), where numerical integration is carried out by the Monte Carlo method with 3000 trials per one realization of the composite at each spectral point. The uncertainty of the Monte Carlo integration is much less than the width of the lines in the corresponding plots (see below). The mean field approximation is calculated from Eq. (39).

The enhancement factors for composites with $N=500$ inclusions in the unit cell for the fill factors $0.001 \leqslant f \leqslant 0.12$ are presented in Fig. 8. The behavior of the enhancement factor in this case is similar to that for the case of nonlinearity in the host (cf. Fig. 5), though the enhancement is appreciably higher. Also, in all of the visible to infrared spectral range there is optical enhancement $|g^{(3)}|>1$ in contrast to Fig. 5. The mean-field theory gives a reasonable agreement with the present computations only for the lowest fill factor presented, $f=0.001$. Similar to the case nonlinear inclusions, as f increases, a peak grows to the red region from the surface plasmon resonance of inclusions dominating the picture at $f=0.001$. At $f \geqslant 0.04$, the mean-field theory fails completely, even on the order of magnitude. This is due to development of the giant fluctuations of local fields introduced in Ref. 27.

To check numerical consistency, we present in Fig. 9 results of the computation of $|g^{(3)}|$ for different numbers of inclusions in the unit cell N (the left panel) and for different numbers of repetitions of the unit cell (the right panel). The main conclusion that one can draw from this figure is that both the number of inclusions and the number of cells are sufficient (the curves shown overlap within their widths for most of the spectral region).

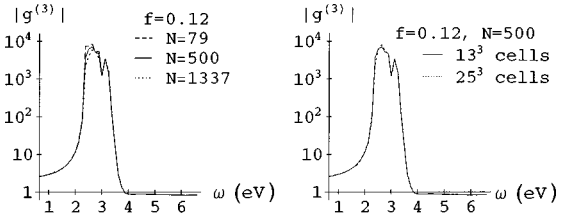

FIG. 9. Magnitude of enhancement coefficient $|g^{(3)}|$ for the fill factor $f=0.12$ and different unit cell sizes $N=79$, 500, and 1337 (left panel) and different numbers of repetition of the unit cell in the composite (right panel). Data are plotted for optically linear inclusions in a nonlinear host. Note the double logarithmic scale.

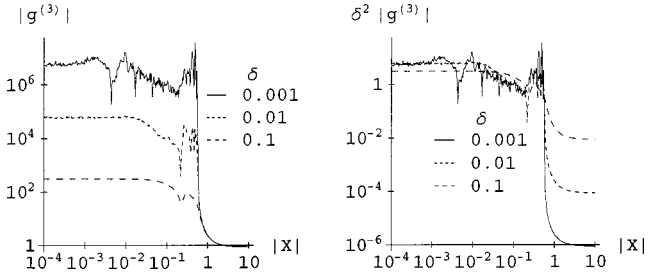

FIG. 10. Same as in Fig. 6, but for the case of a nonlinear host and linear inclusions.

Finally, we discuss whether for the case of nonlinearity in the host there is a scaling in δ similar to that shown in Fig. 6. In Fig. 10 we show spectral dependence of $|g^{(3)}|$ in terms of the spectral variable X and dissipation parameter δ. We conclude that in this case as well, the enhancement factor for $|X|\lesssim 1$ scales as $|g^{(3)}|\approx C\delta^{-2}$. This provides the spectral representation for the nonlinear susceptibility, giving a material-independent description of the results.

In recent experiments,[22] cancellation of $\mathrm{Im}\,\chi^{(3)}$ due to nontrivial consequences of local-field effects has been observed, predicted on the basis of a mean-field theory. In these experiments, both the host and inclusions are optically nonlinear. Correspondingly, our theoretical prediction for the nonlinear susceptibility would be a sum of the corresponding contributions found above and in Sec. III C. All the observations of Ref. 22 are in a good agreement with the mean-field theory of Ref. 20. The reason for such good an agreement is that the fill factor in Ref. 22 is very low, $f=2.2\times10^{-6}$. At such values of f, the present theory predicts the mean-field theory to be completely applicable (cf. the panels for $f=0.001$ in Figs. 5 and 8).

IV. CONCLUSIONS

Let us very briefly summarize the major results obtained without repeating most of the discussion already given above. We have calculated both linear (ε_c) and nonlinear ($\chi_c^{(3)}$) optical susceptibilities of Maxwell Garnett composites in a dipolar spectral theory. The theory is asymptotically exact for composites where typical distances between inclusions are much greater than the sizes of the inclusions. In our range of the fill factors ($0.001\leqslant f\leqslant 0.12$), our computations should have an error of 10% or less. For the sake of comparison, we have also computed these susceptibilities in a mean-field approximation.

Our main goal has been finding nonlinear susceptibilities of composites. However, for the sake of testing our methods, we have also calculated linear responses. The spectral function computed agrees within the expected 10% error with the previous calculations of Ref. 19.

We have suggested a material-independent spectral representation for nonlinear susceptibilities, which is not quite trivial, because the corresponding spectral function depends directly on the dissipation, unlike that for the linear susceptibilites. We have achieved this goal by choosing the spectral variables X and δ, and showing that there is a scaling in δ in the region of optical enhancement.

We conclude that the mean-field approximation does not describe the susceptibilities under consideration in the resonant region where optical absorption is present. For the linear dielectric function, the disagreement of the mean-field approximation (Maxwell Garnett theory) is more significant for the imaginary part, which is understandable, because $\mathrm{Im}\,\varepsilon_c$ is nonzero only the region of optical absorption.

We have found that there is a significant (by several orders of magnitude) enhancement of the nonlinear susceptibility $\chi_c^{(3)}$ in the resonant region. For the nonlinear responses, the mean-field theory is applicable only for very low fill factors ($f\lesssim 0.001$). For larger fill factors, it completely fails to describe the maximum magnitude (even on the order of magnitude) of $\chi_c^{(3)}$ and its spectral contour. The likely cause of this dramatic behavior is the presence of giant spatial fluctuations of local fields[27] related to the long-range nature of the dipole interaction.

ACKNOWLEDGMENTS

The authors are grateful to J. E. Sipe for many useful discussions and participation in the formulation of the problem. We greatly appreciate helpful comments and suggestions by D. Bergman, R. Fuchs, and B. I. Shklovskii. Comments by P. Visscher regarding the treatment of the periodic boundary conditions are gratefully acknowledged.

*To whom correspondence should be addressed. Electronic address: mstockman@gsu.edu; Web site: www.phy-astr.gsu.edu/stockman.

[1] H.A. Lorentz, Wiedem. Ann. **9**, 641 (1880).
[2] J. C. Maxwell Garnett, Philos. Trans. R. Soc. London, Ser. B **203**, 385 (1904); **205**, 237 (1906).
[3] D.A.G. Brugemann, Ann. Phys. (Leipzig) **24**, 636 (1935).
[4] H.A. Lorentz, *Theory of Electrons* (Dover, New York, 1952).
[5] A. Lagendijk, B. Nienhuis, B.A. van Tiggelen, and P. de Vries, Phys. Rev. Lett. **79**, 657 (1997).
[6] P. de Vries, D.V. van Coevorden, and A. Lagendijk, Rev. Mod. Phys. **70**, 447 (1998).
[7] R.G. Barrera, C. Noquez, and E.V. Anda, J. Chem. Phys. **96**, 1574 (1992).
[8] S. Kumar and R.I. Cukier, J. Phys. Chem. **93**, 4334 (1989).
[9] B. Cichocki and B.U. Felderhof, J. Chem. Phys. **90**, 4960 (1989).
[10] D.J. Bergman, Phys. Rev. B **14**, 4304 (1976).
[11] D.J. Bergman, Phys. Rep. **43**, 377 (1978).

[12] D.J. Bergman and D. Stroud, *Properties of Macroscopically Inhomogeneous Media*, edited by H. Ehrenreich and D. Turnbull, Solid State Physics Vol. 46 (Academic Press, Boston, 1992), p.148.
[13] G. Milton, J. Appl. Phys. **52**, 5286 (1981).
[14] R. Fuchs, Phys. Rev. B **11**, 1732 (1975).
[15] R. Rojas and F. Claro, Phys. Rev. B **34**, 3730 (1986).
[16] R. Fuchs and F. Claro, Phys. Rev. B **39**, 3875 (1989).
[17] R. Fuchs, R. Barrera, and J.L. Carrillo, Phys. Rev. B **54**, 12 824 (1996).
[18] V.A. Markel, L.S. Muratov, and M.I. Stockman, Zh. Éksp. Teor. Fiz. **98**, 819 (1990) [Sov. Phys. JETP **71**, 455 (1990)]; V.A. Markel, L.S. Muratov, M.I. Stockman, and T.F. George, Phys. Rev. B **43**, 8183 (1991).
[19] K. Hinsen and B.U. Felderhof, Phys. Rev. B **46**, 12 955 (1992).
[20] J.E. Sipe and R.W. Boyd, Phys. Rev. A **46**, 1614 (1992).
[21] R.J. Gehr, G.L. Fisher, and R.W. Boyd, J. Opt. Soc. Am. B **14**, 2310 (1997).
[22] D.D. Smith, G.L. Fisher, R.W. Boyd, and D.A. Gregory, J. Opt. Soc. Am. B **14**, 1625 (1997).
[23] D. Stroud and P.M. Hui, Phys. Rev. B **37**, 8719 (1988).
[24] R. Rammal, J. Phys. (France) Lett. **46**, L129 (1985).
[25] H. Ma, R. Xiao, and P. Sheng, J. Opt. Soc. Am. B **15**, 1022 (1998).
[26] V.M. Shalaev, M.I. Stockman, and R. Botet, Physica A **185**, 181 (1992).
[27] M.I. Stockman, L.N. Pandey, L.S. Muratov, and T.F. George, Phys. Rev. Lett. **72**, 2486 (1994).
[28] We assume that the polarizability of an *isolated* inclusion particle α_0 is a scalar, i.e., $(\alpha_0)_{\beta\gamma}=\delta_{\beta\gamma}\alpha_0$. Despite this, the polarizability $\alpha^{(a)}$ of the same inclusion in a *composite* is a nontrivial tensor due to loss of the central symmetry owing to disordered nature of the composite.
[29] M.I. Stockman, T.F. George, and V.M. Shalaev, Phys. Rev. B **44**, 115 (1991).
[30] L. D. Landau and E.M. Lifshitz, *Electrodynamics of Continuous Media* (Pergamon Press, New York, 1960).
[31] J. Cullum and R.A. Willoughby, *Lanzcos Algorithms for Large Symmetric Eigenvalue Computations* (Birkhauser, Basel, 1985).
[32] M.P. Allen and D.J. Tildesley, *Computer Simulation of Liquids* (Clarendon Press, Oxford, 1987), Sec. 5.5.
[33] P.B. Johnson and R.W. Christy, Phys. Rev. B **6**, 4370 (1972).
[34] M.I. Stockman, V.M. Shalaev, M. Moskovits, R. Botet, and T.F. George, Phys. Rev. B **46**, 2821 (1992).
[35] B.I. Shklovskii, *Electronic Properties of Doped Semiconductors* (Springer, New York, 1984).
[36] M.I. Stockman, L.N. Pandey, and T.F. George, Phys. Rev. B **53**, 2183 (1996).
[37] M.I. Stockman, Phys. Rev. Lett. **79**, 4562 (1997).
[38] M.I. Stockman, Phys. Rev. E **56**, 6494 (1997).
[39] M.I. Stockman, L.N. Pandey, and T.F. George, in *Nonlinear Optical Materials*, edited by J. V. Moloney, IMA Volumes in Mathematics and its Applications Vol. 101 (Springer-Verlag, New York, 1998), p. 225.
[40] A.V. Butenko, P.A. Chubakov, Yu.E. Danilova, S.V. Karpov, A.K. Popov, S.G. Rautian, V.P. Safonov, V.V. Slabko, V.M. Shalaev, and M.I. Stockman, Z. Phys. D **17**, 283 (1990).